Diesel Engine Cycle to Cycle Feed-forward plus Closed-loop Combustion Control

Preprints, 6th IFAC Conference on
Engine and Powertrain Control, Simulation and Modeling
Tokyo, Japan, August 23-25, 2021

Diesel Engine Cycle to Cycle Feed-forward plus Closed-loop Combustion Control

Loris Ventura * **Andrea Manelli** * **Stefano A. Malan** **

* *Energy Department, Politecnico di Torino, Torino, Italy (e-mail: loris.ventura@polito.it and andrea.manelli@polito.it).*
** *Department of Electronics and Telecommunications, Politecnico di Torino, Torino, Italy (e-mail: stefano.malan@polito.it).*

Abstract: A model-based open-loop compensator has been combined with a cycle to cycle closed-loop controller with the aim of managing engine load and NO_x (Nitrogen Oxides) emission. Both the control strategies employ a virtual sensor realized through a predictive combustion model calibrated on real test bench measurements. Thanks to the virtual sensor no direct in-cylinder pressure measurement is required. Injected fuel quantity and start of injection of the main pulse are regulated to target the desired engine load and NO_x respectively. In the closed-loop control the regulation of the manipulated variables is performed by two separate loops implementing PI and lag regulators, one to control the engine load and the other the NO_x. Both open-loop and closed-loop strategies have been tested separately and then in cooperation between them in order to improve the closed-loop controller time response. Model-in-the-Loop technique was exploited to develop and assess the three control strategies by co-simulation between Simulink and GT-Power executing a fast-running model of a light-duty FPT F1C Euro VI diesel engine. Simulations show promising results and real-time capacity, therefore the strategies are suitable for successive implementation on the real engine through rapid prototyping.

Keywords: Engine modelling and control, Model-based control, Virtual sensors, Feed-forward compensation, Model-in-the-loop simulation.

1. INTRODUCTION

New forms of mobility like electric or hydrogen powered vehicles, at present time, do not have adequate infrastructures for the energy production and distribution to support their diffusion, see Finesso et al. (2018). For this reason diesel Internal Combustion Engines (ICEs) will remain the prime propulsion system for not less that 20-30 years especially in light and heavy-duty sectors.

In order to meet continuously more stringent engine pollutant emission regulations, car manufacturers developed innovative technologies to be provided to gasoline and diesel ICEs. About diesel ICEs, Exhaust Gas Recirculation (EGR) and Variable Geometry Turbochargers (VGTs), see Baratta et al. (2015), together with related control methodologies, see Ventura et al. (2019), Ventura and Malan (2020), high pressure common rail injection systems, see Ferrari et al. (2018), innovative combustion concepts and advanced control, see D'Ambrosio et al. (2018), Malan and Ventura (2018), represent some of these technologies. Additional possibilities are offered by alternative fuels such as Compressed Natural Gas (CNG) and biofuels, see Di Iorio et al. (2012), and engine hybridization. With the introduction of these technologies the degree of complexity and the number of actuators in diesel engines vastly grew. In this context the adoption of advanced model-based algorithms offers several advantages in managing this complexity, achieving lower pollutant emissions, even without the need of dedicated sensors, see Finesso et al. (2017a), Finesso et al. (2017b), Finesso et al. (2017c).

Present day Engine Control Units (ECUs) are capable of executing complex algorithms in real-time thus allowing in-cylinder combustion control through sensor-based and model-based controllers that have proven to be more effective than map-based control approaches, see Yin et al. (2020), Albin et al. (2015). Paper Yin et al. (2020) illustrates a combustion and air-path model of a partially premixed combustion engine to be used in a model predictive controller. The engine load, represented by gross Indicated Mean Effective Pressure (IMEP) was regulated by the main injection duration using a specific linear feedback. Two pilot injections were controlled separately depending on engine load and speed. The control algorithm presented in Albin et al. (2015) through a nonlinear optimization of a cost function at every time step minimizes the fuel consumption and produced pollutants. The algorithm manipulates main injection fuel quantity, Start Of Injection (SOI) and EGR rate.

On the other hand sensor-based controls require direct sensor measurements in the combustion chamber, so they are commonly called in-cylinder techniques. Paper Chung et al. (2016) reports an in-cylinder pressure-based real-time combustion control that, by means of main injection quantity and timing and pilot injection quantity, reduces combustion dispersions in diesel engines by regulating the IMEP, the crank angle location corresponding to 50% of

Mass Fraction Burned (MFB50) and the maximum value of Heat Release Rate (HRR_{max}). Work Willems et al. (2010) presents a in-cylinder pressure-based control system for conventional diesel combustion with high EGR levels. The controller makes use of a physically based combustion model that exploits the in-cylinder pressure measurements to predict NO_x and soot. In Luo et al. (2015) a systematic approach for a cycle to cycle combustion controller design with multi-pulse fuel injection is considered. In work Carlucci (2014) a control function integrated in the basic ECU in-cylinder pressure-based combustion control was developed and tested on a EURO 6-compliant vehicle.

In present work a model-based open-loop controller has been combined with a cycle to cycle closed-loop controller, which are capable of tuning the main pulse fuel mass quantity (q_{main}) and hydraulic SOI to achieve desired targets of NO_x and engine Brake Mean Effective Pressure (BMEP) for a 3.0L FPT F1C diesel engine for light-duty applications. The main novelty of this study consists in the exploitation of model-based controllers that do not need any in-cylinder measurement thanks to the embedded predictive combustion model described in Finesso et al. (2016). Implementation and testing of the controllers was accomplished by means of Model-in-the-Loop (MiL) simulation, through the coupling of Simulink environment with a GT-Power fast running model of the engine. This work is a preliminary step to verify the functionality of the controllers before the implementation in the real engine, which will be carried out in the near future.

2. PROBLEM DEFINITION

Present section gives a description of the engine, the combustion model and the adopted test procedure.

2.1 Engine

A GT-Power model of a FPT F1C 3-litre EURO VI diesel engine was used. The engine is endowed with short route EGR, VGT, Exhaust flap, Intercooler and EGR cooler. Table 1 reports its main specifications while its layout is shown in Fig. 1.

Table 1. FPT F1C Engine Main Specifications

Engine type	FPT F1C Euro VI diesel engine
Number of cylinders	4
Displacement	2998 cm^3
Bore x stroke	95.8 x 104 mm
Rod lenght	160 mm
Compression ratio	17.5 : 1
Valves per cylinder	4
Turbocharger	VGT type
Fuel injection system	High Pressure Common Rail

2.2 Combustion model

Combustion models, generally fed with the in-cylinder measured pressure signal, are used in controllers to evaluate the heat produced by the combustion and consequently the calculation of the produced work and pollutants.

Here the combustion process is described through a physically based, mean-value model. It simulates the in-cylinder

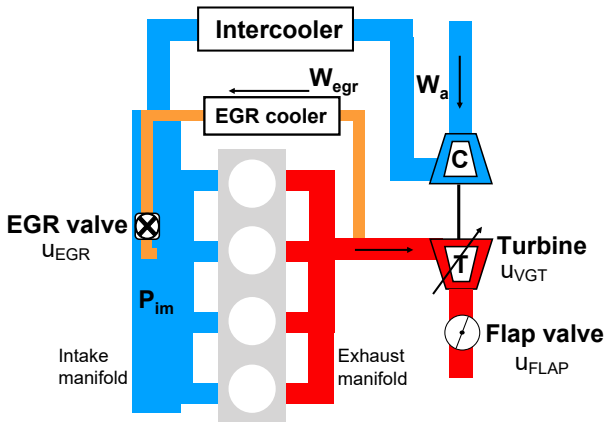

Fig. 1. FPT F1C Engine layout.

pressure, HRR, and related combustion metrics (e.g. MFB50). The model is based on the enhanced accumulated fuel mass approach, in which the rate of chemical energy released by the fuel, in the form of heat, at any time instant t, is proportional to the energy related with the in-cylinder accumulated fuel mass. Through a heat transfer model the net energy released is calculated and then used in the evaluation of the in-cylinder pressure trace. Once the pressure trace is available all the related metrics, such as gross IMEP, can be retrieved. Subtracting to gross IMEP the friction and pumping losses the BMEP is finally obtained. Equation (1) correlates the accumulated fuel mass to the command variable, q_{main}.

$$q_{main} = m_{f,m} = \int_{t_{SOI,m}}^{t_{EOI,m}} \dot{m}_{f,m}(\tau) d\tau \qquad (1)$$

NO_x estimation is given by equation (2) as the sum of two terms: nominal mapped emission, $NO_{x,map}$ and the deviation, δ, of NO_x emission compared to the nominal map values. The latter term is function of the variations of MFB50 and oxygen, and of the ratio between the intake manifold pressure and main pulse fuel mass.

$$NO_x = NO_{x,map}(RPM, BMEP) + \\ + \delta NO_x(\delta MFB50, \delta O_2, \frac{p_{IMF}}{q_{main}}, NO_{x,map}) \qquad (2)$$

The combustion model was calibrated through test bed measurements taken on the engine at hand. All data needed as inputs to the virtual sensor come from the engine ECU and commonly installed sensors on production engines. This choice allows not to further complicate the engine layout installing in-cylinder pressure sensors. Furthermore the model is suitable for real-time implementation on rapid prototyping devices. Model complete details and explanation can be found in Finesso et al. (2016).

2.3 Model in the loop

The controllers, implemented in Simulink environment, were tested in co-simulation with GT-Power running a Fast-Running engine model. Model-in-the-loop test points are represented by rectangles in Fig. 2 over the F1C engine map. For each of these test points an increasing/decreasing load ramp at fixed engine speed has been performed. As an example, Fig. 3 illustrates the test ramp employed in the leftmost rectangle of Fig. 2, at 1150rpm.

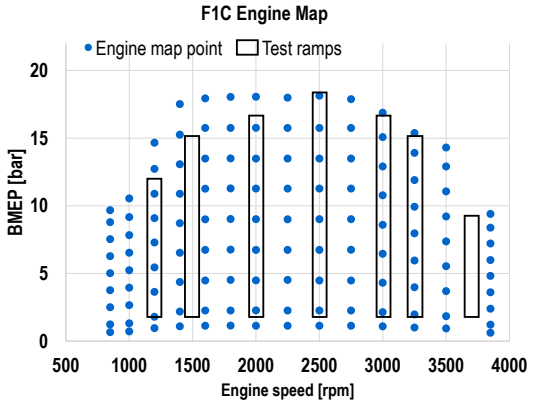

Fig. 2. Engine map with test points.

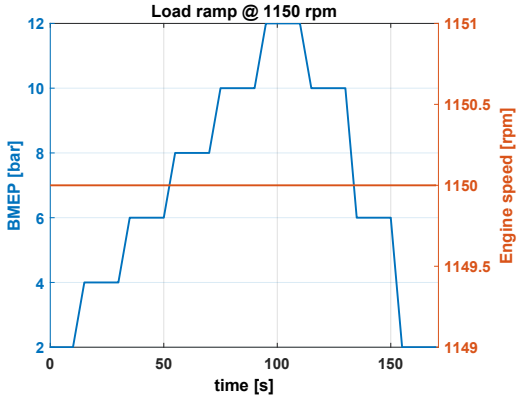

Fig. 3. Engine load (BMEP) test ramp at 1150 rpm.

3. CONTROL ARCHITECTURE

The controller objective is to regulate the engine BMEP and engine out NO_x pollutant emission. Main injection fuel quantity, q_{main}, and SOI are respectively used as manipulated variables. This choice is justified by the fact that the sensitivity of BMEP to q_{main} is much greater than the sensitivity to SOI_{main}, and the sensitivity of NO_x to SOI_{main} is greater than the sensitivity to q_{main} (when the error on the BMEP is small and q_{main} is not far from the reference value assumed to produce target BMEP). However both SOI_{main} and q_{main} influence BMEP and NO_x emissions. This is taken into account in the combustion model as can be seen from equations (1) and (2). In equation (1) SOI_{main} defines the lower limit of the integral while in equation (2) BMEP, that implicitly is related to q_{main}, is used as independent variable for the map of NO_x.

The control architecture is composed by two sections depicted in Fig. 4: an open-loop regulator and a closed-loop feedback controller with the add of a virtual sensor. The architecture allows the use of only one of the two, or both working together. Anyway, when only the closed-loop action is used, a feed-forward action is still present (not in figure) and it is carried out by means of steady state maps that, given the actual values of engine speed and BMEP, provide the nominal values for the two manipulated variables. Those maps are usually built using data obtained from experimental campaigns on the real engine.

The open-loop computes a cycle by cycle feed-forward correction, through an iterative procedure, for each firing

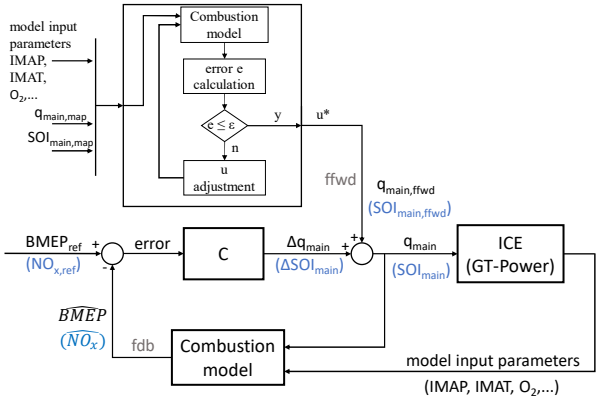

Fig. 4. Controlled system layout.

cylinder, starting from initial values of SOI_{main} and q_{main} given by the ECU maps. In order to adjust the control variables a cycle-based integral control was applied. The iterative procedure stops when the difference between the predicted values and targets fall under a predefined thresholds ϵ. The integral control for q_{main} and SOI_{main} is presented in equations (3) and (4).

$$q^j_{main,i+1} = q^j_{main,i} + K^j_{BMEP,i} \frac{Err^j_{BMEP,i}}{S^j_{BMEP,i}} \tag{3}$$

$$SOI^j_{main,i+1} = SOI^j_{main,i} + K^j_{NO_x,i} \frac{Err^j_{NO_x,i}}{S^j_{NO_x,i}} \tag{4}$$

Superscript j defines the combustion event while subscript i the algorithm iteration. K is a proportional correction factor, Err denotes the error and S is a sensitivity factor between considered manipulated variable and output.

The closed-loop controller is made of two separate branches dedicated to the BMEP and NO_x control. The BMEP branch is regulated by a PI controller, equation (5):

$$C(s) = \frac{2.75(s + 181.8)}{s}, \tag{5}$$

whereas the NO_x branch is regulated by a lag compensator, equation (6):

$$C(s) = \frac{-0.04(s + 0.5)}{(s + 0.02)(s + 1)}. \tag{6}$$

The *Combustion model* described in section 2.2 is used as a virtual sensor to provide the feedback of estimated BMEP and NO_x. Individual cylinder management by the closed-loop controllers results in a total of eight compensators, two each cylinder.

Both open-loop and closed-loop controllers in regulating the injection timing apply the same correction, ΔSOI_{main}, also to the pilot injections. In other words, the train of pilot and main injections is moved rigidly.

The major difference between the two loops regards the inputs. In particular, the inputs of the open-loop controller come from the steady state maps while the closed-loop

operates with the actual variables that the engine used in the previous working cycle.

SOI regulation loop is the most critical one: it must ensure combustion stability avoiding engine damaging, especially considering idle or full load conditions. Furthermore, combustion model numerical predictions in some operating condition may express a non-physically significant behavior. Small variations in the SOI actuation result in a sensible change in the predicted NO_x. Mathematically this will cause a visible oscillation in the NO_x prediction while the SOI oscillates between two close values physically not achievable and distinguishable on the real engine.

To cope with these oscillations, avoiding SOI continuous variation, a quantization interval of 0.1deg has been added to the closed-loop controller. A proper value for this quantization will be set during experiments in the engine test rig. Moreover due to safety reasons closed loop outputs are saturated to ±6mg of fuel and ±6deg of SOI angle.

4. RESULTS

The control system performances were checked in co-simulation between Simulink and the GT-Power model representing the engine. For the sake of brevity only three transient load ramps relative to low, medium and high engine speeds are here discussed. However similar results have been obtained on the remaining four ramps. Speed has not been varied because the control targets the engine BMEP, standing for torque load, and it has been preferred to separate the two variation of engine speed and BMEP.

Each ramp was performed with four different configurations of the control structure:

(1) open and closed-loop controls disabled, steady state map feed-forward only;
(2) only open-loop control enabled, in place of steady state map;
(3) only closed-loop control enabled, with steady state map feed-forward;
(4) both open and closed-loop enabled.

Figs. from 5 to 10 plot the results of these four configurations respectively in black, red, blue and green.

The load target is set by the ramp profile (one example was given in Fig. 3) while the NO_x target is provided by a steady state map function of engine speed and load. Δq_{main} and ΔSOI_{main} are the outputs of the two control loops: a positive Δq_{main} indicates that more fuel will be injected; a positive ΔSOI_{main} causes the SOI to retard, that is to move it towards the Top Dead Center.

Before discussing the results, note that the ideal situation would be to have zero NO_x emissions, corresponding to a positive NO_x error, but this would cause the deterioration of the engine overall performance and emission trade off, e.g., increase of particulate matter production. For this reason it is needed to maintain the not null NO_x target.

Low speed (1150rpm) load ramp results for the Δq_{main} control loop are reported in Fig. 5 while the ones for the ΔSOI_{main} loop are reported in Fig. 6. By looking at the BMEP error, Fig. 5a, the use of steady state maps without any control, black line, causes an important

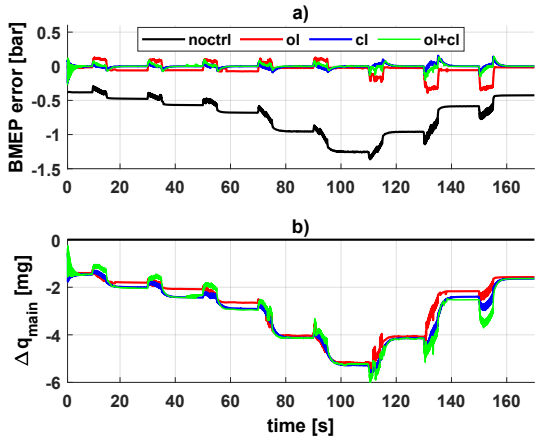

Fig. 5. Load ramp at 1150 rpm:
a) BMEP error; b) Δq_{main} correction.

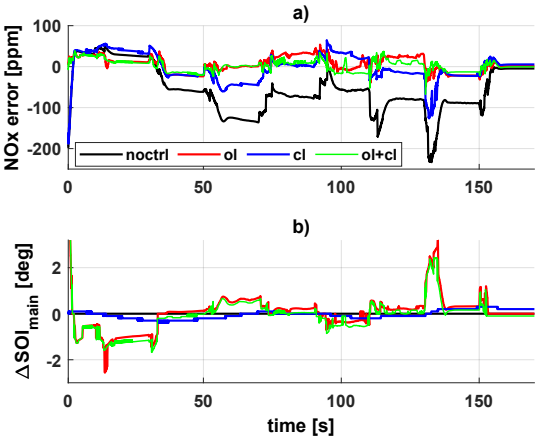

Fig. 6. Load ramp at 1150 rpm:
a) NO_x error; b) ΔSOI_{main} correction.

deviation from the reference value. From this figure it is clearly visible how the open and closed control loops, red and blue lines respectively, are effective in constraining the error between ± 0.1bar. When the open and closed-loop controllers are combined, green line, the behavior of the two is merged causing a better performance. By looking at the fuel quantity correction, Δq_{main}, the three tracks corresponding to the thee controller configurations are very similar, in all the three cases the fuel to be injected is decreased compared to the one derived from steady state maps, Fig. 5b. In the case of both open and closed-loop controllers enabled the correction is given by the summation of the two contributes. The open-loop accounts for the majority of the correction while the closed loop thanks to the integral action effectively avoids offsets. NO_x and ΔSOI_{main} are shown in Fig. 6. The sole open-loop control, red line, notably reduces the NO_x error compared to the map-based SOI actuation shown in black. Compared to the closed-loop controller, blue line, the open-loop expresses a better performance. This is because the open-loop controller is faster than the closed-loop. Combining the two controllers the overall performance improves decreasing the NO_x error and removing some oscillations in the ΔSOI_{main} output.

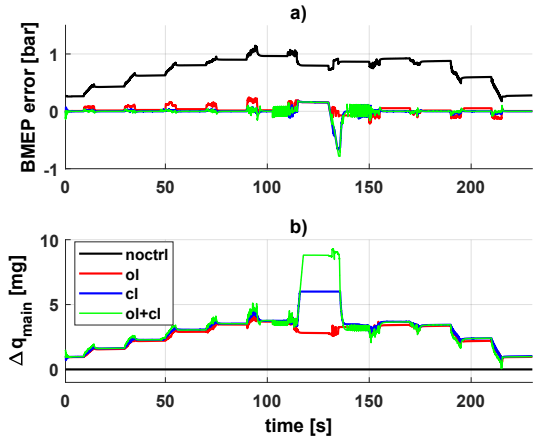

Fig. 7. Load ramp at 2500 rpm:
a) BMEP error; b) Δq_{main} correction.

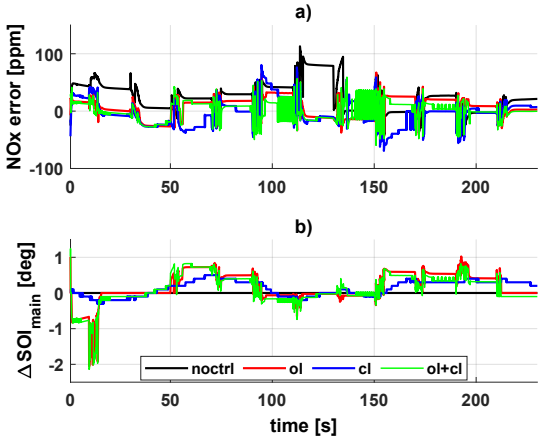

Fig. 8. Load ramp at 2500 rpm:
a) NO_x error; b) ΔSOI_{main} correction.

Figs. 7 and 8 show the results for the load ramp at medium speed (2500rpm). In Fig. 7, where the BMEP error (a) and the main pulse injected fuel correction (b) are reported, it is possible to see the effectiveness of the use of the open and closed loop controllers both able to reduce the error compared to the map-based control (black line). Between the two controllers the open-loop regulation avoids the undershoot at time $t = 130s$ offering a more stable behavior. This undershoot is caused by the closed-loop control that in transients provides an excessive fuel correction reaching $6mg$, Fig. 7b. This problem is accentuated when combining the two controllers as can be seen from the green line. In Fig. 8 the NO_x error (a) and the SOI correction for the main pulse (b) are reported; also in this case the performance of the open-loop controller in regulating the NO_x are better compared with the closed-loop though in some transient it expresses sharp transitions in the SOI regulation, Fig. 8b. Combining the two strategies, green line, originates the best performance. The oscillations visible in Fig. 8a are the results of small variation in the SOI regulation, $0.1deg$, that on the real engine will be filtered out by the physical quantization of the SOI command.

Figs. 9 and 10 report high speed (3850rpm) load ramp results for the two control loops respectively. The steady

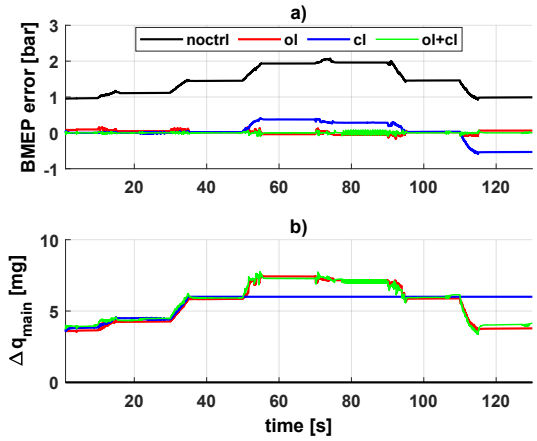

Fig. 9. Load ramp at 3850 rpm:
a) BMEP error; b) Δq_{main} correction.

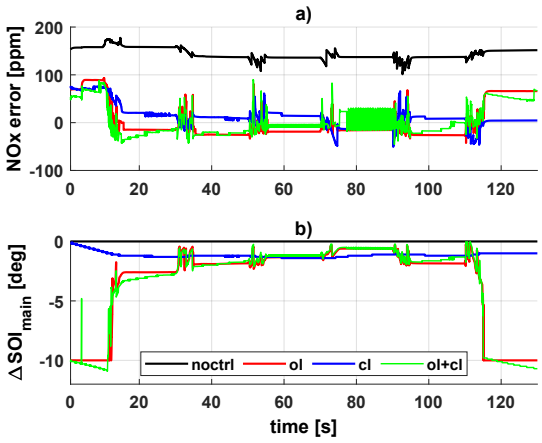

Fig. 10. Load ramp at 3850 rpm:
a) NO_x error; b) ΔSOI_{main} correction.

state map causes a large deficit of BMEP, Fig. 9a - black line, that reaches $2bar$ at the maximum load request. The introduction of the closed-loop control, blue line, improves the tracking of the reference with the error reaching $0.39bar$ in the high load phase and $-0.55bar$ in the final part of the ramp starting from time $t = 115s$. q_{main} control reduces this error to a maximum of $0.42bar$. Instead with the sole open-loop controller active, red line, the error is reduced to a maximum of $0.15bar$. With both the controller active, green line, also the offset are eliminated providing a better tracking of the BMEP reference. The oscillations visible in Fig. 9a are due to the influence of the small variation of SOI but their amplitude has no physical meaning. Also considering the NO_x in Fig. 10a the presence of the sole closed-loop control, blue line, reduces the error compared with the map-based control, black line, which in turn is outperformed by the open-loop one, red line. Combining the two controller the overall performance is increased, green line. The corresponding actuation for the SOI, Fig. 10b, shows that the closed-loop control is the more relaxed one providing a uniform control action, blue line. The open-loop control expresses some oscillation in the transient phases of the ramp and in the two ends, at low load, greatly vary the SOI trying to reduce error. However in these regions, since they are

rarely visited during normal operating conditions of the engine, the SOI should be saturated to preserve engine integrity. Combining the two controllers, green line, it is visible that the open-loop has a predominant contribution over the SOI regulation.

Performance indexes as Root Mean Square Error (RMSE) and mean error percentage related to the four configurations tested on the three ramps at 1150, 2500 and 3850rpm show that the map-based control offers poor performance with an RMSE of 0.77, 0.75 and 1.50bar respectively for BMEP and 79, 35 and 144ppm for the NO_x. Alone, the open-loop controller offers better results compared to the closed-loop one in terms of RMSE and worse considering mean error percentage. Combining the two reduces the RMSE to 0.02, 0.09 and 0.02bar on the BMEP while for the NO_x it drops to 14, 15, 31ppm. In this configuration the mean error percentage over the BMEP is at maximum 0.02% and 2.5% for the NO_x.

5. CONCLUSIONS

Two combustion control strategies, open-loop and closed-loop, have been combined to manage engine BMEP and NO_x emissions through q_{main} and SOI. The main novelty of the developed approach consists in the adoption of a combustion model as virtual sensor. This model does not need any in-cylinder pressure measurement for its predictions, it only exploits ECU available signals. Model-in-the-loop, realized through co-simulation between Simulink and GT-Power environments, performing increasing/decreasing ramps at constant speed, allowed to validate the controller functionality. Results have shown that the controller is effective in achieving a stable and efficient control of both BMEP and NO_x emissions. The controller is very accurate concerning BMEP control, while some oscillations occur in NO_x control. These oscillations are mainly related to the variability of the implemented combustion model for feedback information. Future activities will focus on tests on the real engine of the developed controller and comparison with its sensor-based alternative through actual feedback of in-cylinder pressure and engine out NO_x provided by two dedicated sensors. Moreover a suitable quantization interval and filtering function will be evaluated to cope with the NO_x oscillations problem.

ACKNOWLEDGEMENTS

The authors want to thank profs. S. d'Ambrosio and R. Finesso (Energy Department, Politecnico di Torino) for their valuable help in developing and revising this work.

REFERENCES

Albin, T., Ritter, D., Zweigel, R., and Abel, D. (2015). Hybrid multi-objective MPC for fuel-efficient PCCI engine control. In *2015 European Control Conf.*

Baratta, M., Finesso, R., Misul, D., and Spessa, E. (2015). Comparison between internal and external EGR performance on a heavy duty diesel engine by means of a refined 1d fluid-dynamic engine model. *SAE Int. J. Engines*, 8.

Carlucci, A.*et al.*. (2014). Advanced closed loop combustion control of a LTC diesel engine based on in-cylinder pressure signals. *Energy Conversion and Management*, 77.

Chung, J., Min, K., Oh, S., and Sunwoo, M. (2016). In-cylinder pressure based real-time combustion control for reduction of combustion dispersions in light-duty diesel engines. *Applied Thermal Engineering*, 99.

D'Ambrosio, S., Gaia, F., Iemmolo, D., Mancarella, A., Salamone, N., Vitolo, R., and Hardy, G. (2018). Performance and emission comparison between a conventional Euro VI diesel engine and an optimized PCCI version and effect of EGR cooler fouling on PCCI combustion. Technical report, SAE Technical Paper.

Di Iorio, S., Beatrice, C., Guido, C., Napolitano, P., Vassallo, A., and Ciaravino, C. (2012). Impact of biodiesel on particle emissions and DPF regeneration management in a Euro 5 automotive diesel engine. Technical report, SAE Technical Paper.

Ferrari, A., Mittica, A., Pizzo, P., and Jin, Z. (2018). PID controller modelling and optimization in CR systems with standard and reduced accumulators. *International Journal of Automotive Technology*, 19(5).

Finesso, R., Marello, O., Misul, D., Spessa, E., Violante, M., Yang, Y., Hardy, G., and Maier, C. (2017a). Development and assessment of pressure-based and model-based techniques for the MFB50 control of a Euro VI 3.0 L diesel engine. *SAE Int. J. of Engines*, 10(4).

Finesso, R., Marello, O., Spessa, E., Yang, Y., and Hardy, G. (2017b). Model-based control of BMEP and NO_x emissions in a Euro VI 3.0 L diesel engine. *SAE Int. J. of Engines*, 10(5).

Finesso, R., Misul, D., Spessa, E., and Venditti, M. (2018). Optimal design of power-split HEVs based on total cost of ownership and CO_2 emission minimization. *Energies*, 11(7).

Finesso, R., Spessa, E., and Yang, Y. (2016). Development and validation of a real-time model for the simulation of the heat release rate, in-cylinder pressure and pollutant emissions in diesel engines. *SAE Int. J. of Engines*, 9(1).

Finesso, R., Spessa, E., Yang, Y., Conte, G., and Merlino, G. (2017c). Neural-network based approach for real-time control of BMEP and mfb50 in a Euro 6 diesel engine. Technical report, SAE Technical Paper.

Luo, X., Wang, S., de Jager, B., and Willems, F. (2015). Cylinder pressure-based combustion control with multi-pulse fuel injection. *IFAC-PapersOnLine*, 48(15).

Malan, S.A. and Ventura, L. (2018). Air-path control for a prototype PCCI diesel engine. In *2018 26th Mediterranean Conference on Control and Automation*.

Ventura, L. and Malan, S.A. (2020). NLQR control of high pressure EGR in diesel engine. In *2020 20th Int. Conf. on Control, Automation and Systems*.

Ventura, L., Finesso, R., Malan, S.A., d'Ambrosio, S., and Manelli, A. (2019). Model-based design of closed loop controllers of the air-path in a heavy duty diesel engine. *AIP Conference Proceedings*, 2191(1).

Willems, F., Doosje, E., Engels, F., and Seykens, X. (2010). Cylinder pressure-based control in heavy-duty EGR diesel engines using a virtual heat release and emission sensor. Technical report, SAE Technical Paper.

Yin, L., Turesson, G., Tunestål, P., and Johansson, R. (2020). Model predictive control of an advanced multiple cylinder engine with partially premixed combustion concept. *IEEE/ASME Trans. on Mechatronics*, 25(2).